Weak Lensing and DM Subhalos in Very Nearby Galaxy Clusters

T. Futamase,
Kyoto Sangyo University
1st July. 2016 @ IFT, Univ. Madrid

Collaborator:
N. Okabe (Hiroshima U) 、Y.Okura(Riken)

Context

- New Techniques in Weak Lensing Analysis
- Motivation
- Results
- Future

Importance of GL in Cosmology

- **Direct Method of Mass Detection**

depends on gravity only, does not need any empirical relation

between luminosity and mass

independent on dynamical state and composition

complementary to other traditional observation such as

X-ray(hot gas), visible and infrared light(stars)

- **Dependence on geometry and expansion of the Universe**
- **Lensing by Large scale structure affects any cosmological observables**

Noise may become signal of LSS

- **Natural telescope**

Shear measurement in weak lensing

$$\beta = \theta - \partial_\theta \psi(\theta)$$

$$\Rightarrow \frac{\delta\beta}{\delta\theta} = (1-\kappa)\begin{pmatrix} 1 & 0 \\ 0 & 1 \end{pmatrix} - \begin{pmatrix} \gamma_1 & \gamma_2 \\ \gamma_2 & -\gamma_1 \end{pmatrix}$$

convergence shear

$$\kappa(\vec{\theta}) \equiv \frac{\Sigma(\theta)}{\Sigma_{cr}}$$

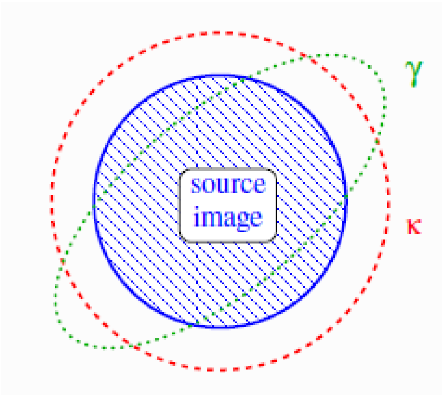

Ellipticity and shear

$$\varepsilon^{(\mathrm{lensed})} \approx \varepsilon^{(\mathrm{intrinsic})} + a\,\gamma$$ in linear order

depends on the def. of ellipticity

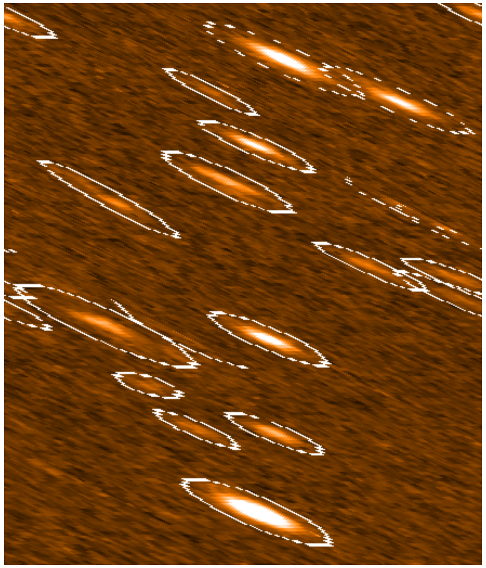

After averaging

$$<\varepsilon^{(\mathrm{lensed})}>(\vec{\theta}) = a <\boldsymbol{\gamma}>(\vec{\theta}) + O\left(\frac{\sigma_{\mathrm{int}}}{\sqrt{N}}\right)$$

However the lensed image is not the observed image due to atmospheric turbulence and so on

$$I^{(Obs)}(\theta) = \int d^2\theta' I^{(lens)}(\theta') P(\theta - \theta')$$

Point Spread Function(PSF)

- Another problem is that

Difficulties in Weak Lensing Analysis

There will be a great progress weak lensing observation from ground as well as from space near future , but it does not automatically means the great progress in the accuracy of weak lensing analysis.

- Many systematic errors are not yet fully controlled

  PSF correction
- We can use only high S/N object

PSF correction

Galaxies: Intrinsic galaxy shapes to measured image:

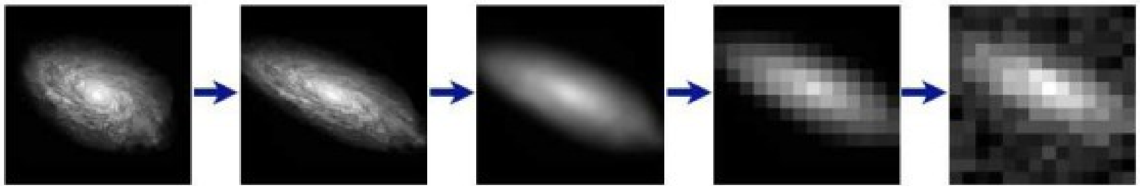

Bridle et al.2008

$I^{(lens)}$ $\qquad$ $I^{(Obs)}$

$$I^{(Obs)}(\theta) = \int d^2\theta' I^{(lens)}(\theta') P(\theta - \theta')$$

Point Spread Function(PSF)

Stars: Point sources to star images:

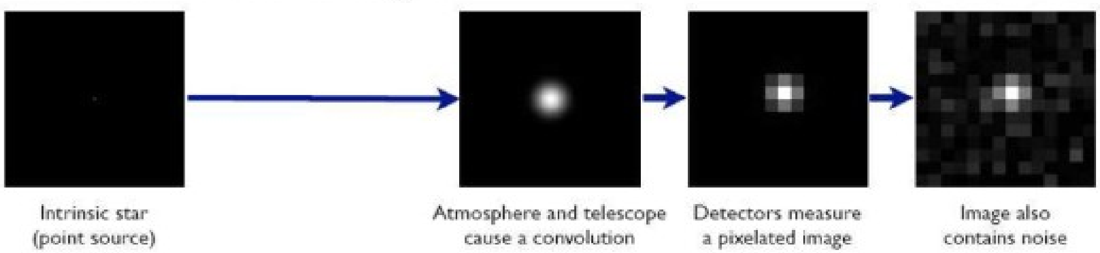

P is measured at the position of star

$$I^{star}(\theta_{star}) = \int d^2\theta' \delta(\theta') P(\theta_{star} - \theta') = P(\theta_{star})$$

Typical number density

$$n_{star} \approx 1 \ \text{arcmin}^{-2}$$

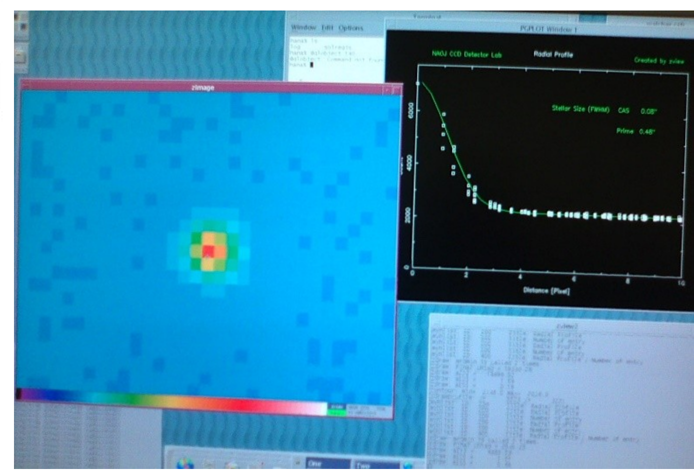

Star image in the best seeing (0.48") in Hawaii

We have introduced new techniques in weak lensing analysis(Y.Okura &T.F, 2014,2015)

- New PSF correction free from any bias

$$\hat{I}^{(Ob)}(k) = \hat{I}^{(Lensed)}(k)P(k)$$

If P has the same elliticity with I^lensed, then I^Ob has the same ellipticity

The idea is to smear the original PSF again by an appropriate function R to make re-smeared PSF to have the same ellipticity with the lensed galaxy

$$\hat{P}^{(R)}(\vec{k}) = \hat{P}(k)\hat{R}(\vec{k})$$

$$\hat{I}^{(R)}(\vec{k}) = \hat{I}^{(Obs)}(k)\hat{R}(\vec{k}) = I^{(Lensed)}(\vec{k})\hat{P}(\vec{k})\hat{R}(\vec{k})$$

$$= I^{(Lensed)}(k)\hat{P}^{(R)}(k)$$

Choose R to make $\hat{I}^{(R)}(k)$ and $\hat{P}^{(R)}(k)$ to have the same ellipticity

For this to happen we iteratively solve the equation to find P^(R)

$$\hat{R}(\vec{k}) = \frac{\hat{P}^{(R)}(\vec{k})}{P(k)}$$

New method of PSF correction(ERA)

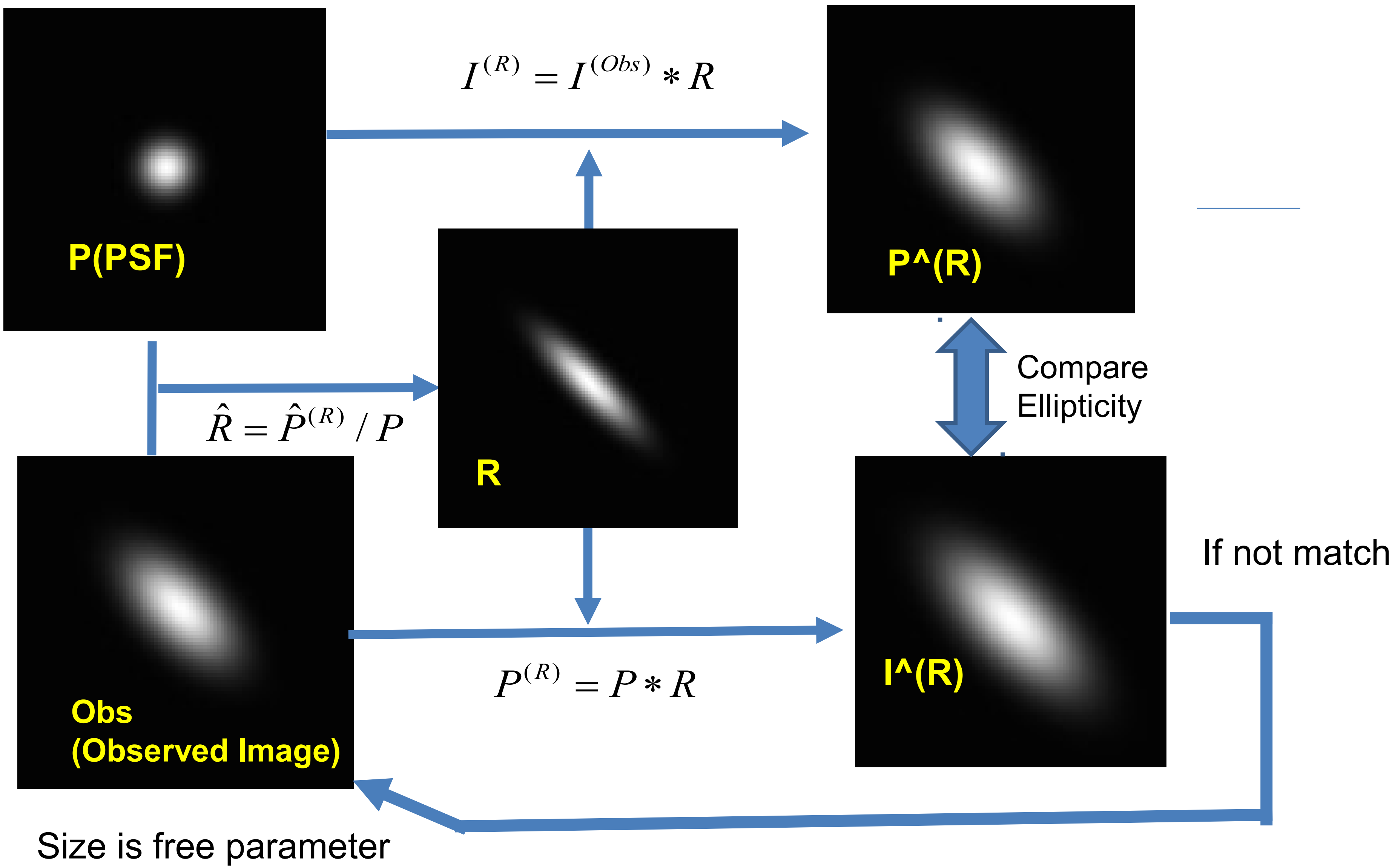

Iteration result using Simulation

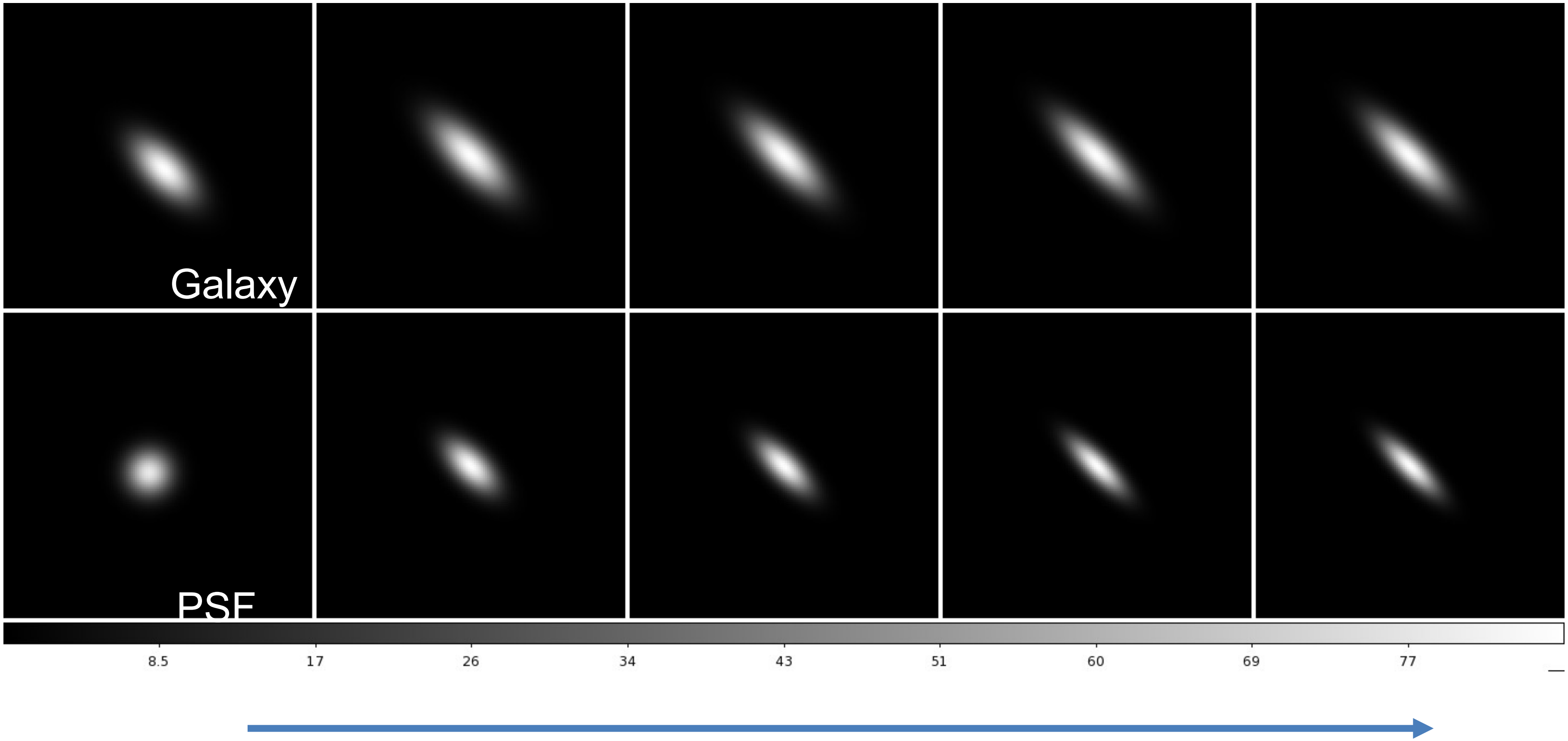

Comparison between Regaussian in HSC pipeline and ERA

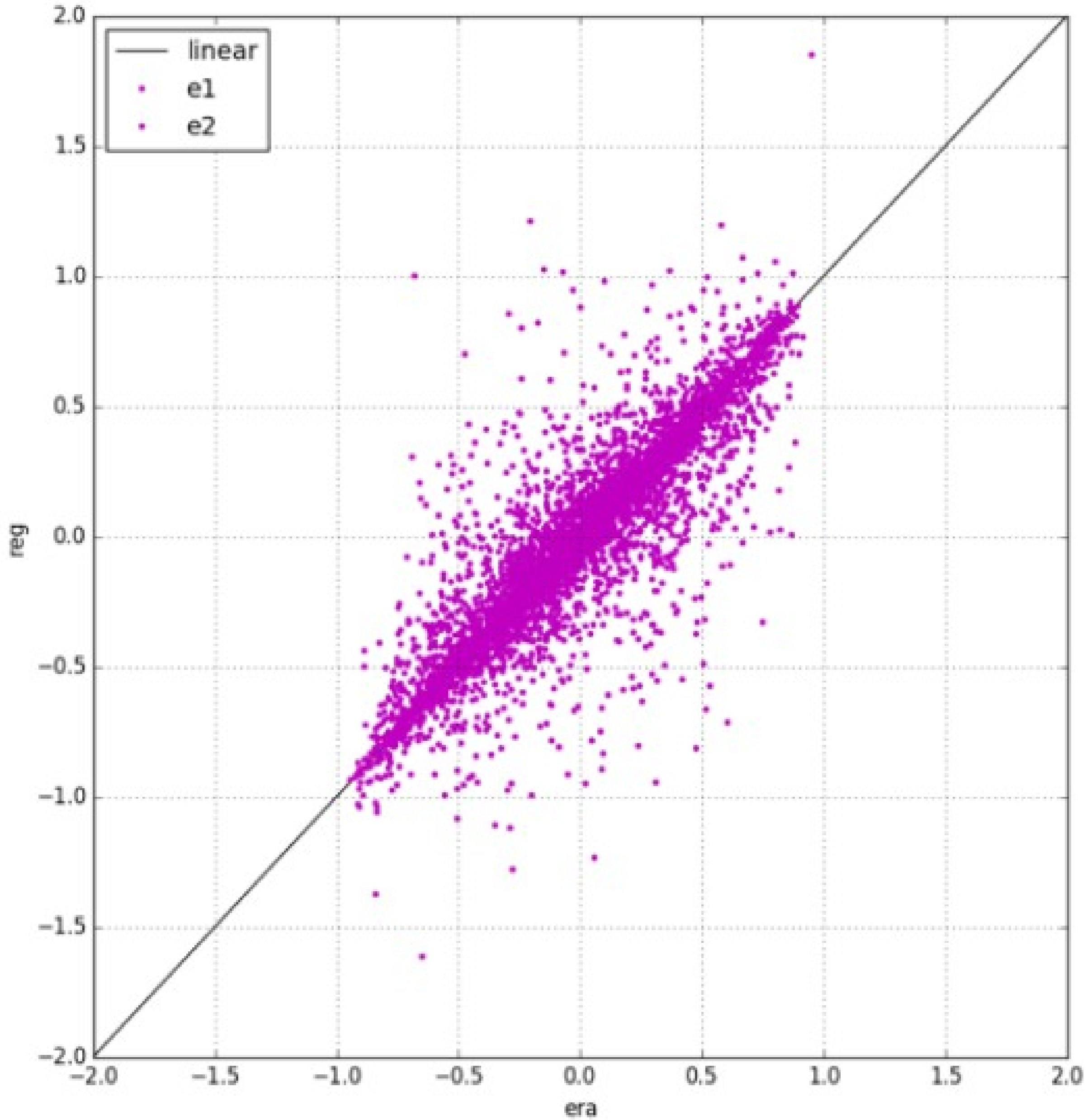

- New spin 2 ellipticity

Usual spin 2 ellipticity

$$\varepsilon = \int d^2\theta \ \mathrm{I}(\theta)\left[\left(\theta_1^2 - \theta_2^2\right) + i\theta_1 \theta_2\right]$$

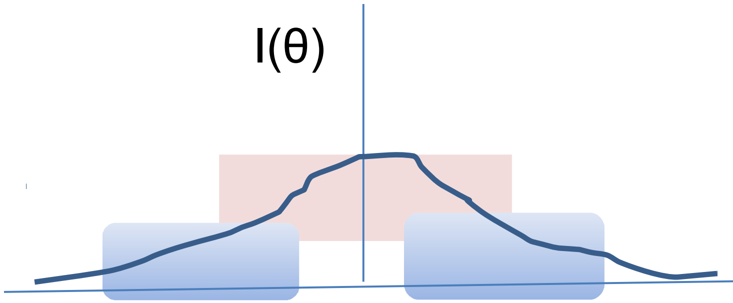

Newly defined spin 2 ellipticity

$$\varepsilon = \int d^2\theta \ \frac{\mathrm{I}(\theta)}{\theta_1^2 + \theta_2^2}\left[\left(\theta_1^2 - \theta_2^2\right) + i\theta_1 \theta_2\right]$$

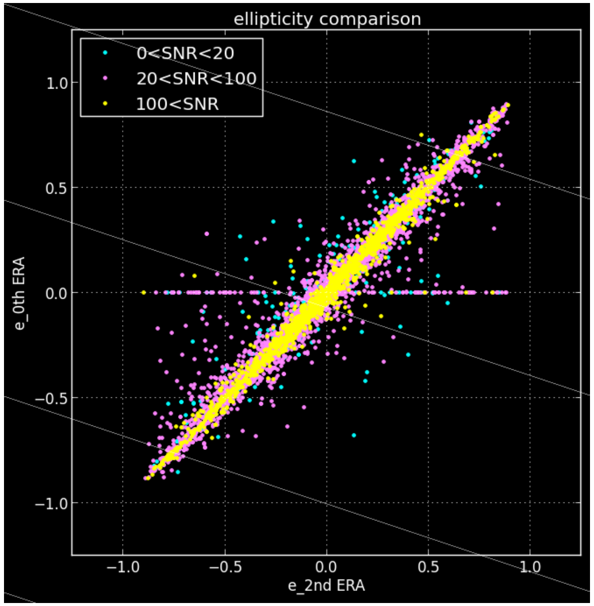

Motibation of our study

Comparison of Field of View

1999/01/28
Subaru First Light

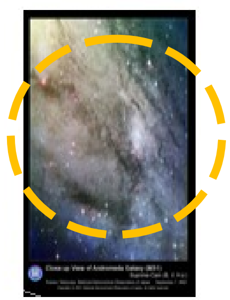

2001/09/07
Suprime-Cam

2013/07/31
Hyper Suprime-Cam

Fields

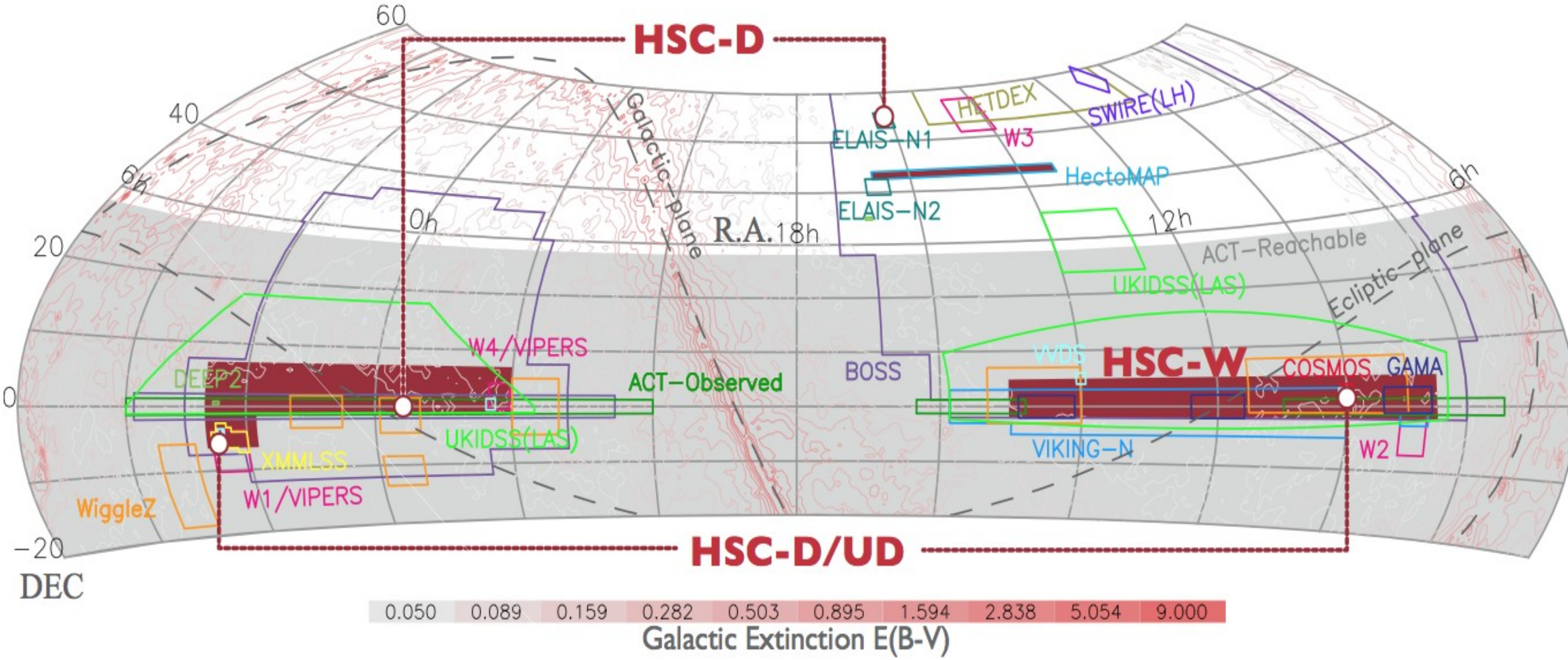

Figure 11: The location of the HSC-Wide, Deep (D) and Ultradeep (UD) fields on the sky in equatorial coordina A variety of external data sets and the Galactic dust extinction are also shown. The shaded region is the reg accessible from the CMB polarization experiment, ACTPol, in Chile.

Wide:~640, ~680, ~55(spec-z) deg^2

g, r :10 min, i: 20 min; z, y: 20 min.

Weak Lensing Study of Clusters

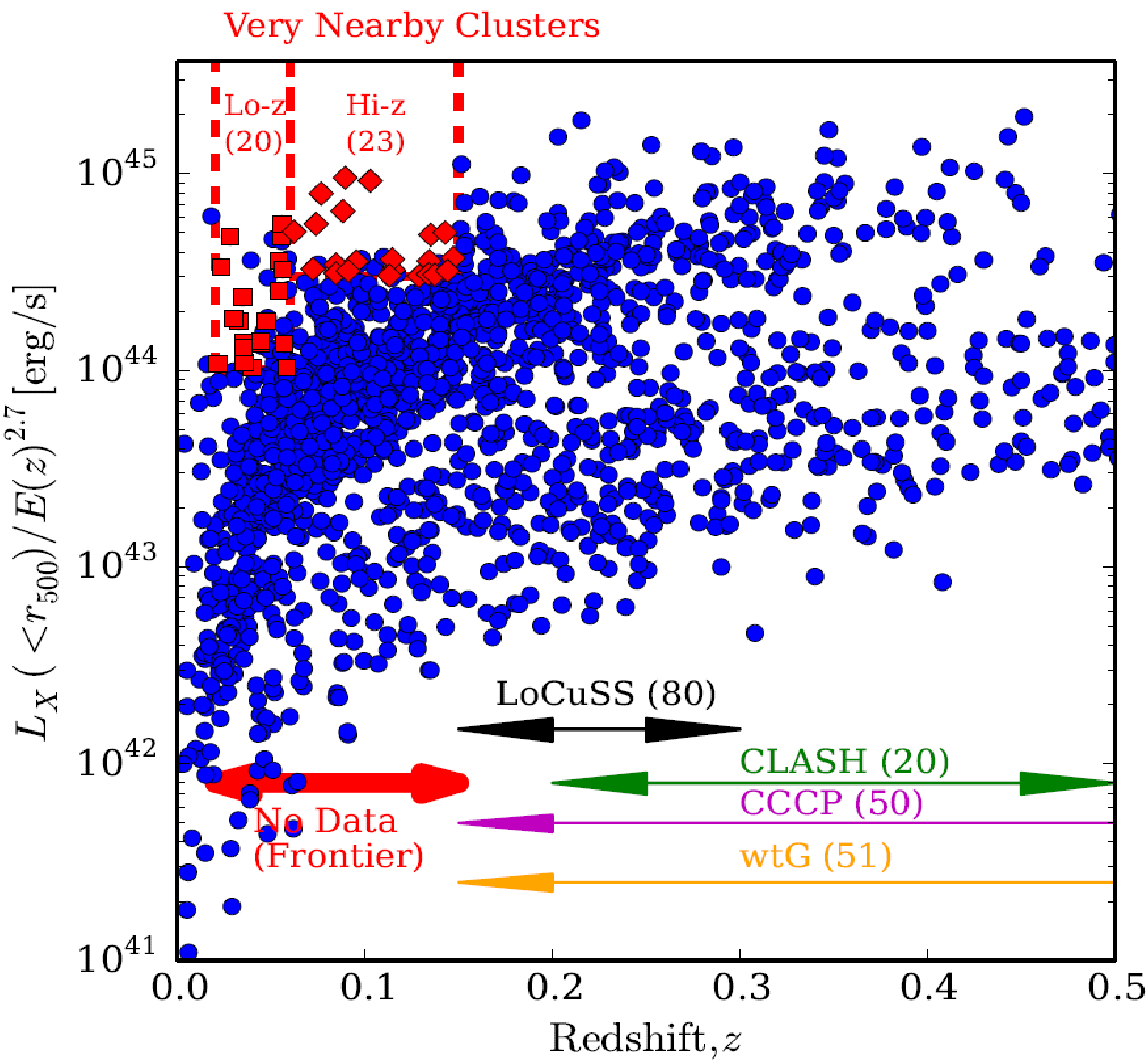

CDM Structure Formation Scenario

- **Small CDM halos with baryon in the center form first and then they gether together to form more larger CDM halos**
- **Galaxies and galaxy clusters contain many CDM subhalos**
- **Theory predicts the averaged mass profile of main halo and mass function of subhalos**
- **Observation of CDM halos allows us to test SDM structure formation scenario and DM property**

Why Nearby cluster?
for example Coma (z=0.0236)

One of the most massive and compact cluster in our neighbor

- Huge apparent size (~3 square degree~5Mpc^2)

  Even subhalos have sizes larger than angular resolution

  of weak lensing

  1 arcmin~28 kpc for h=0.7 at z=0.0236
- Huge number of background galaxies is available which compensates low lensing efficiency and improve statistical error
- Hyper Suprime-Cam

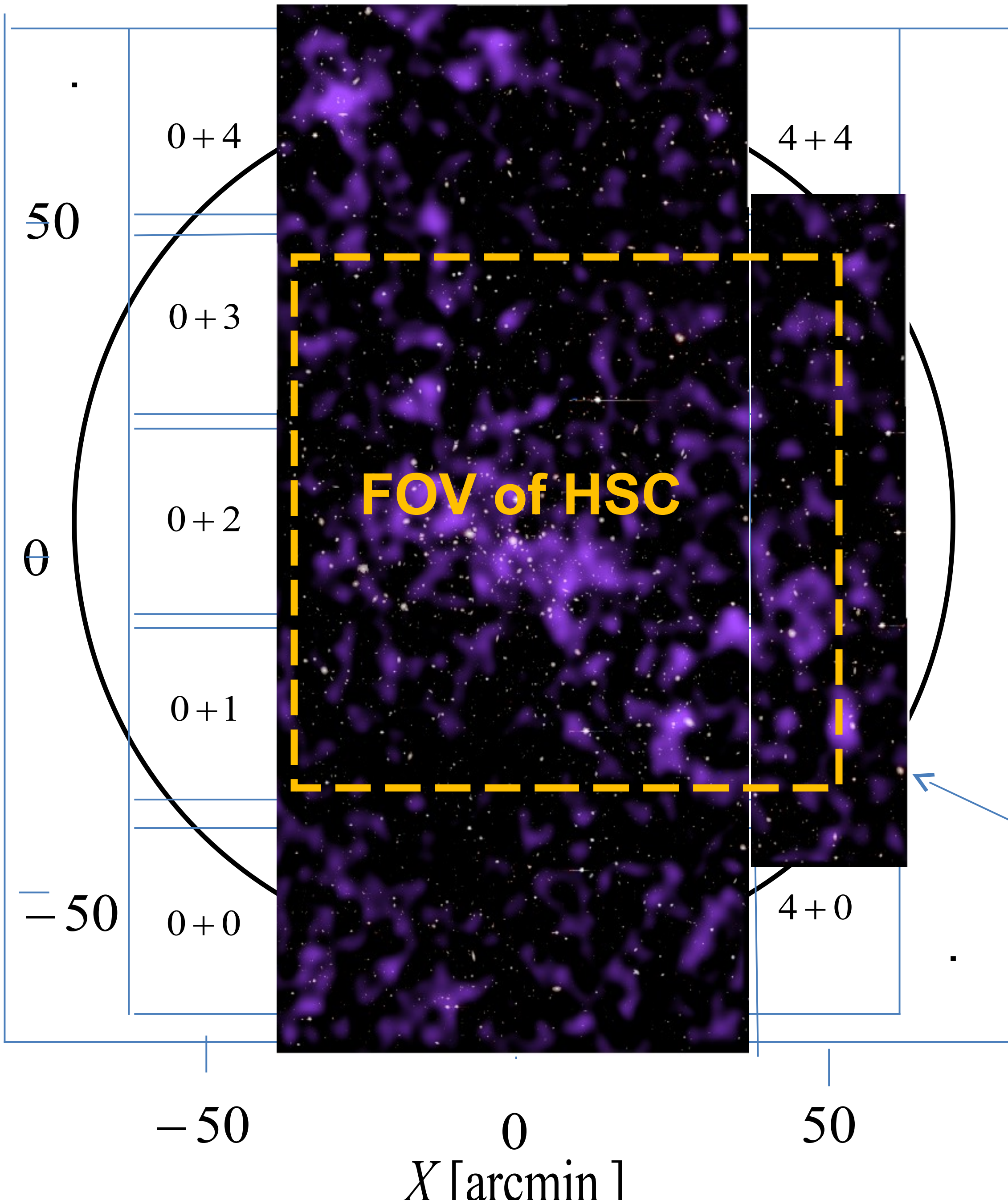

2 full nights in March 2011
2 square degree surcey
seeing ~0.7"

Number density of background galaxies ~50/arcmin^2
18 pointings in Rc band(24.5min) and V band (13.8min)

N.Okabe,T.F, M.Kajisawa, R.Kuroshima (2013)

Projected mass distribution

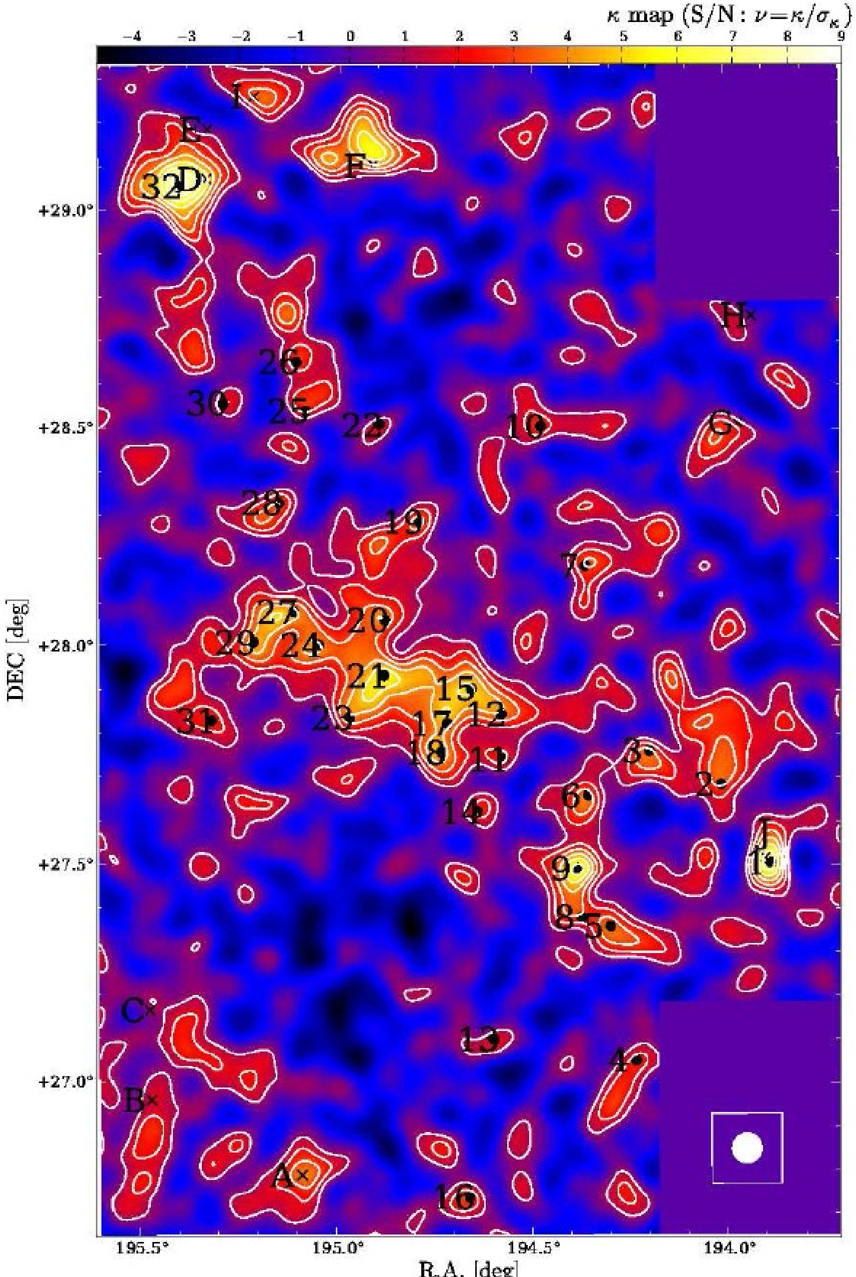

Smoothing scale =4'

In unit of significance $\nu \equiv \kappa / \sigma_\kappa$

$\sigma_\kappa \approx 7.7 \times 10^{-3}$: mass reconstruction error

$\nu > 3$ are defined as peaks

Known background systems

ID[a]	Name	$z_{\rm phot}$[b]
A	MaxBCG J195.08820+26.78870	0.162
B	GMBCG J195.47315+26.95810	0.219
C	MaxBCG J195.47907+27.16429	0.208
D	GMBCG J195.34791+29.07201	0.189
E	MaxBCG J195.34617+29.18616	0.170
F	NSC J125939+290715	0.189
G	GMBCG J193.96542+28.51557	0.257
H	MaxBCG J193.92901+28.76123	0.259
I	SDSSCGB 06685	0.183
J	WHL J125535.3+273104	0.418

Correspondence between DM subhalos and galaxy groups

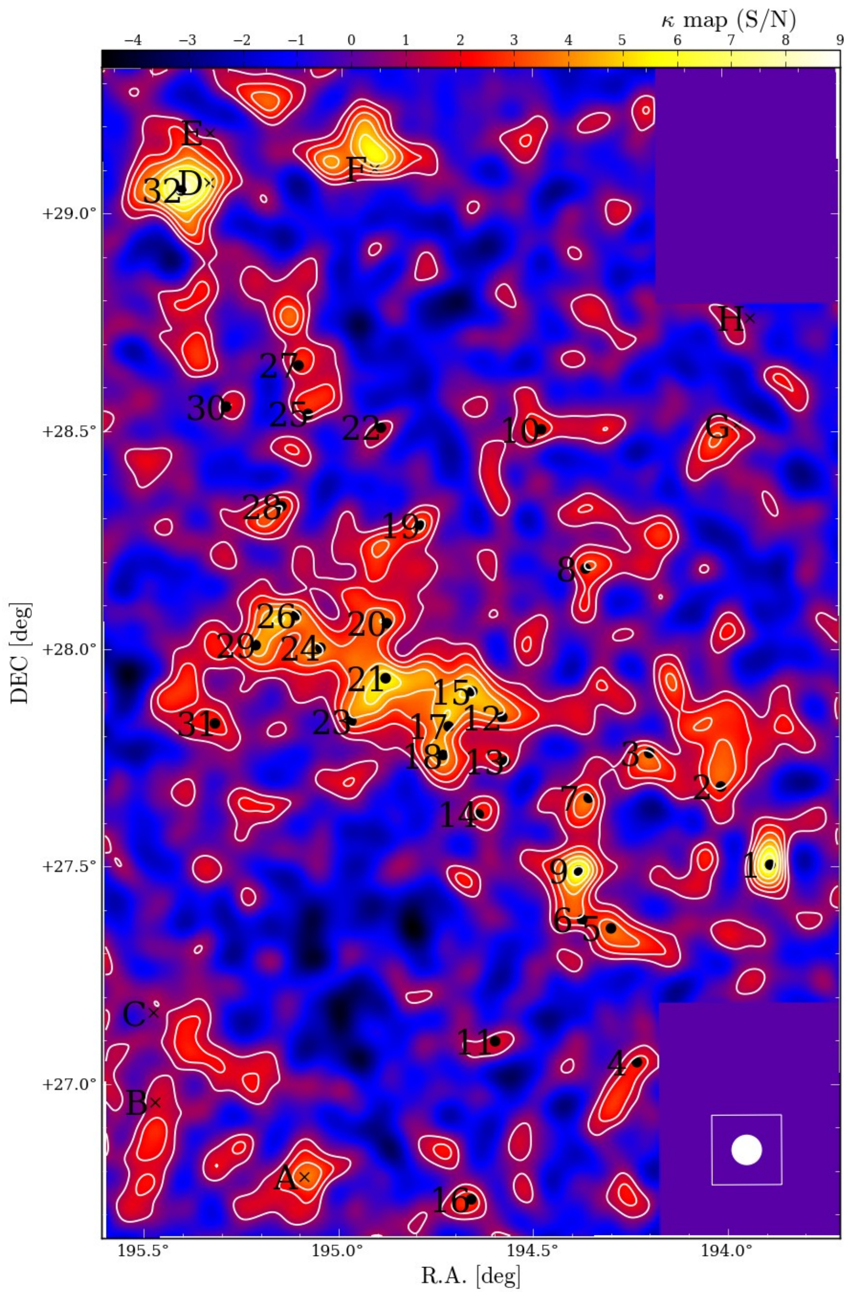

ID[a]	M_{2D}[c] $10^{12}h^{-1}M_{\odot}$	ν[d]	Representative galaxies[e]
1[†]	15.42 ± 2.79	5.98	NGC4807
2	8.79 ± 4.69	3.55	NGC4816 Group[♯]
3	3.71 ± 1.08	4.61	SDSS J125645.42+274638.0
4	2.89 ± 1.08	3.51	SDSS J125647.00+270324.9
5	5.00 ± 2.34	3.86	2MASX J12571076+2724177
6	2.52 ± 1.27	4.45	G12 Group[‡]
7	5.99 ± 2.84	3.80	UGC08071, 2MASX J12572841+2810348
8	1.87 ± 0.73	3.54	2MASX J12573148+2723048
9	12.11 ± 2.52	6.45	NGC4839 Group[♯], G4 Group[♮], NGC4842, X-ray subhalo[♭♭]
10	3.24 ± 0.75	3.42	2MASX J12575392+2829594
11	4.13 ± 0.85	4.03	2MASX J12581922+274543
12	2.02 ± 0.78	3.87	SDSS J125818.20+275054.5
13	2.70 ± 0.77	3.61	2MASX J12581552+2705137
14	4.51 ± 1.27	3.53	NGC4853
15	2.96 ± 1.44	6.90	NGC4839 Group[♯]
16	5.03 ± 1.06	4.19	SDSS J125839.93+264534.2
17	3.13 ± 0.74	4.94	G9 Group[♮], SA 1656-030[♭]
18	6.48 ± 2.03	4.47	G8 Group[♮]
19	4.66 ± 1.26	4.74	SDSS J125914.99+281503.6
20	2.90 ± 1.58	4.16	2MASX J12593141+2802478
21	4.29 ± 1.06	7.23	NGC4874(cD),part of G1 Group[♮], X-ray subhalo 2[♯♯]
22	4.50 ± 1.90	3.54	2MASX J12594129+2830257
23	3.75 ± 1.04	4.26	J194.9353+27.83393[‡], SA 1656-054[♭],X-ray subhalo 3[♯♯]
24	5.20 ± 2.40	4.71	NGC4889(cD),part of G1 Group[♮] X-ray subhalo 1[♯♯]
25	3.86 ± 0.95	3.93	2MASX J13002268+2834285
26	2.75 ± 0.79	4.43	SDSS J130037.14+283950.9
27	4.28 ± 1.74	6.24	SDSS J130030.95+280630.2,part of G7 Group[♮]
28	5.70 ± 1.68	3.68	NGC4896
29	3.64 ± 1.30	4.31	NGC 4908, NGC 4908 Group
30	3.12 ± 0.66	4.03	SDSS J130114.96+283118.3
31	2.97 ± 1.42	3.41	G4 Group[♮], NGC4919
32[††]	45.95 ± 7.57	8.35	G15 Group[♮],IC 4088,2MASX J13014399+2859587

Mass and Luminosity(R-band and X-ray) Distribution

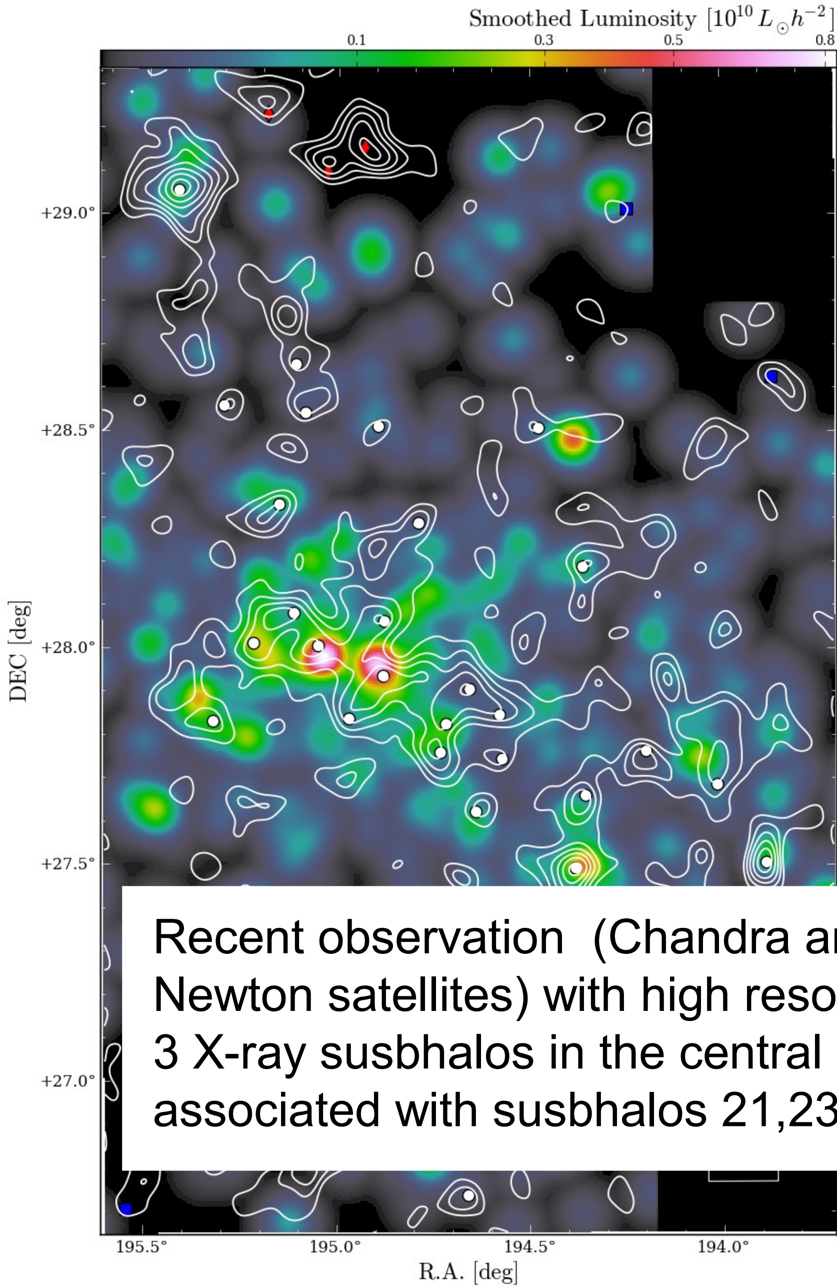

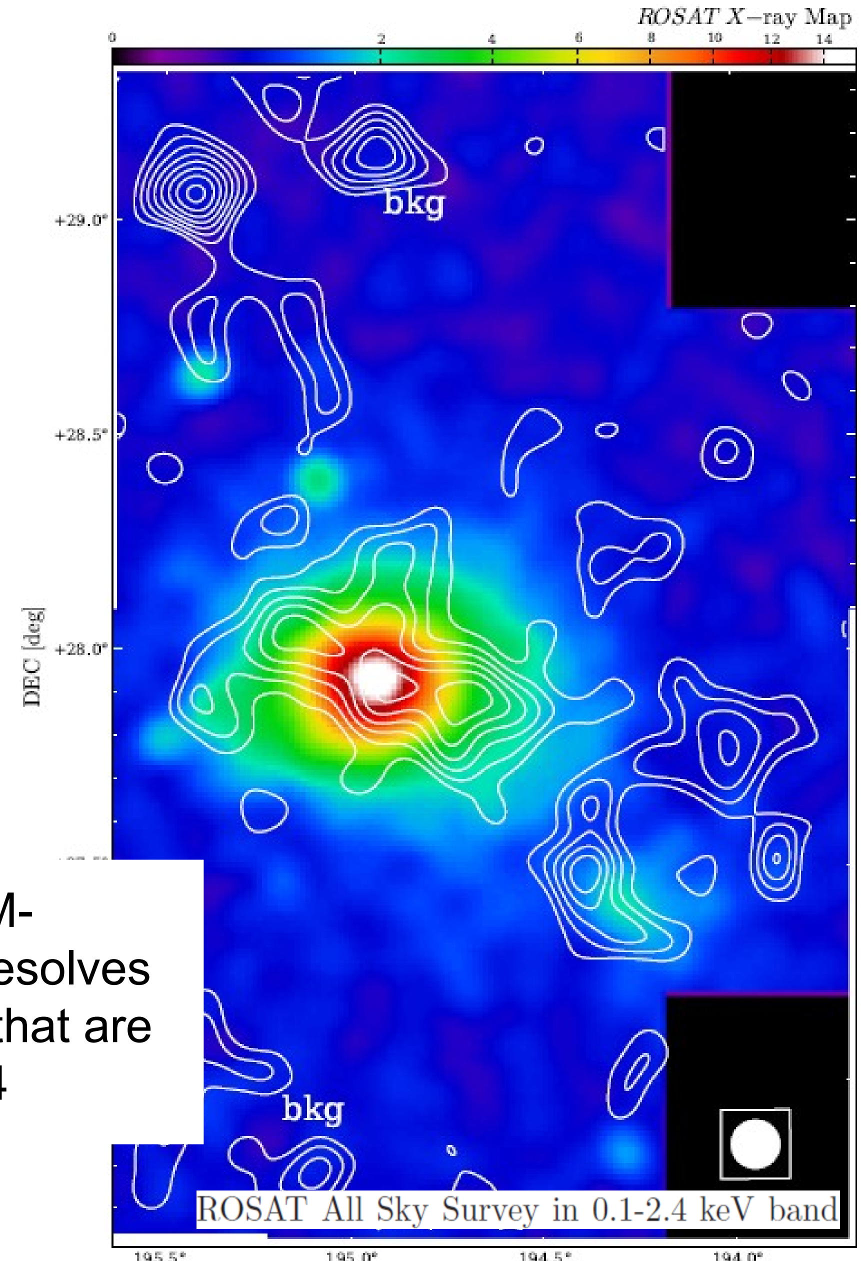

Recent observation (Chandra and XMM-Newton satellites) with high resolution resolves 3 X-ray susbhalos in the central region that are associated with susbhalos 21,23 and 24

Follow-up X ray observation by Suzaku

PROPERTIES OF THE COMA CLUSTER SUBHALOS.

ID[a]	M_{2D}^{b} $10^{12}\ h^{-1}\ M_{\odot}$	M^{c} $10^{12}\ h^{-1}\ M_{\odot}$	r_t^{d} arcmin	(R.A., decl.)[e] J2000.0	N_H^{f} $10^{19}\ \mathrm{cm}^{-2}$	Distance[g] Arcmin/r_{500}
1	15.42 ± 2.79	$14.26^{+2.37}_{-2.53-5.55}$	$3.86^{+0.14}_{-0.19}$	$12^h55^m34^s.5, +27^\circ31'33.7''$	8.6	61.8/1.42
2	8.79 ± 4.69	-	-	$12^h56^m03^s.8, +27^\circ47'20.8''$	8.7	51.6/1.18
32	45.95 ± 7.57	$47.75^{+5.81}_{-5.81-13.42}$	$9.21^{+0.74}_{-0.83}$	$13^h01^m41^s.0, +29^\circ03'14.4''$	9.5	71.2/1.63

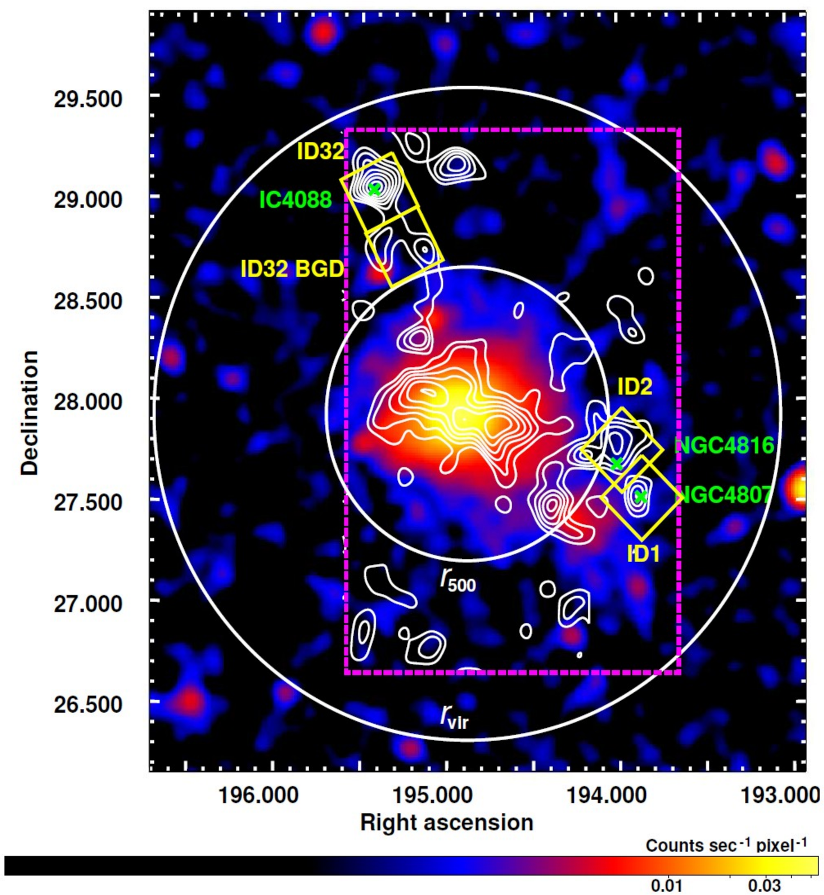

arXive:1504.03044
T.Sasaki, K. Matsushita, K.Sato and N. Okabe

ID1,2 and 32

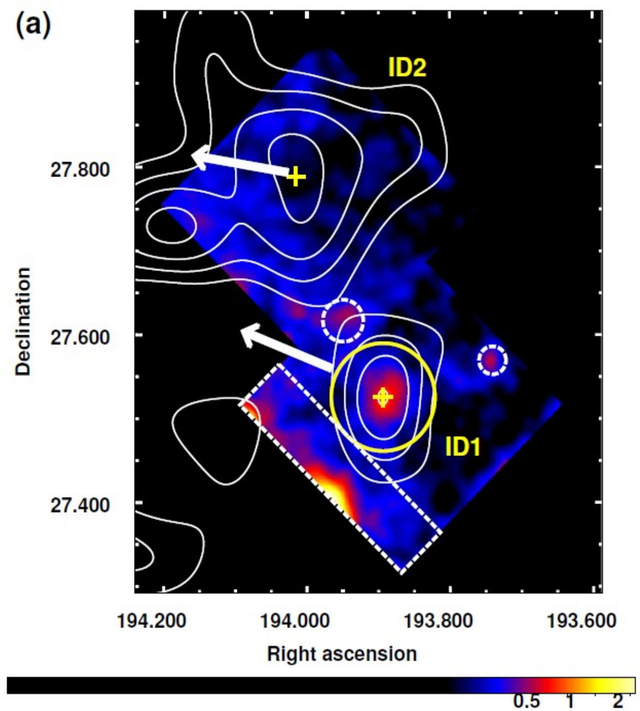

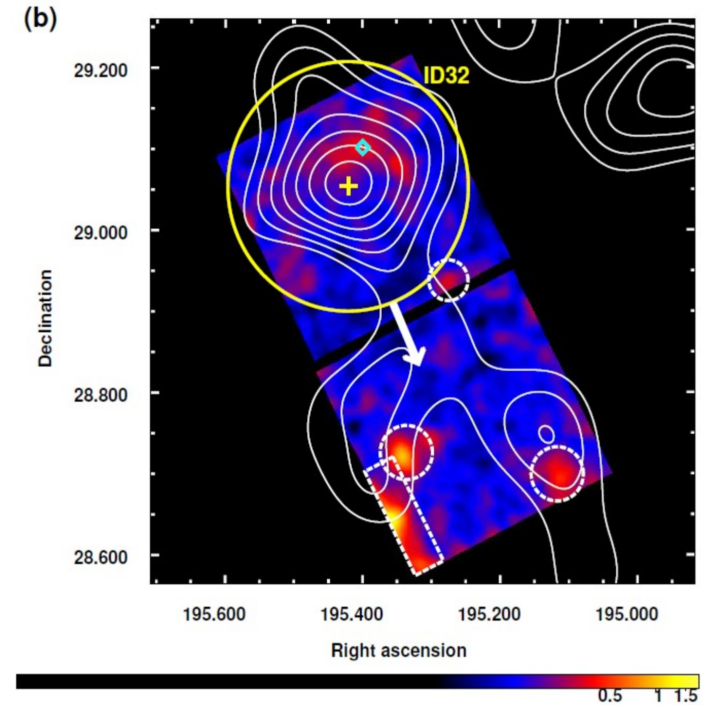

The projected surface brightness profiles

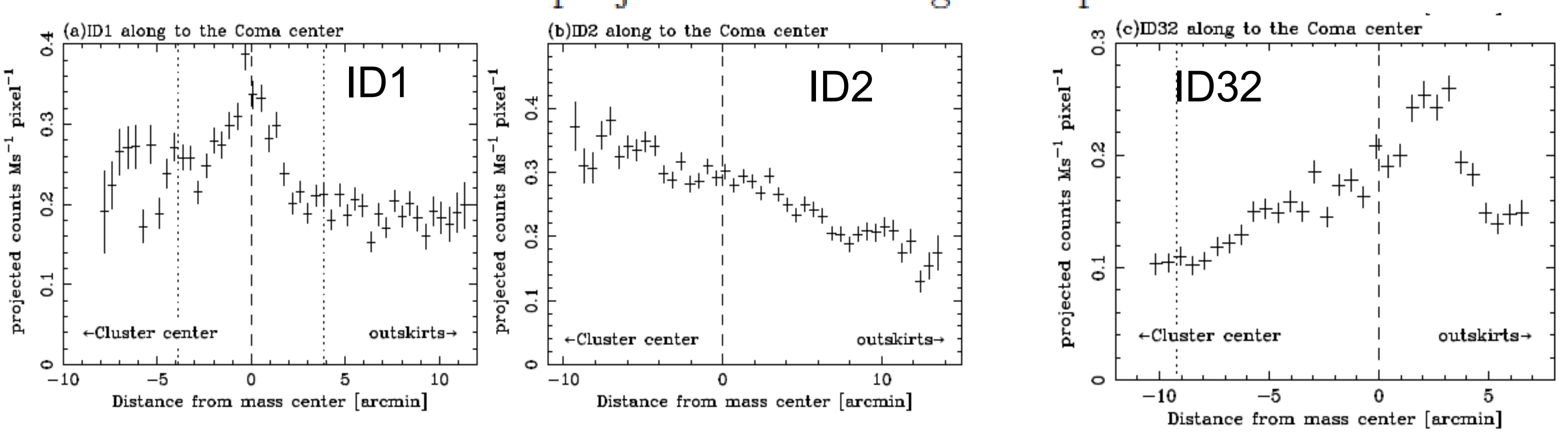

The subhalo gas mass versus weak-lenisng mass

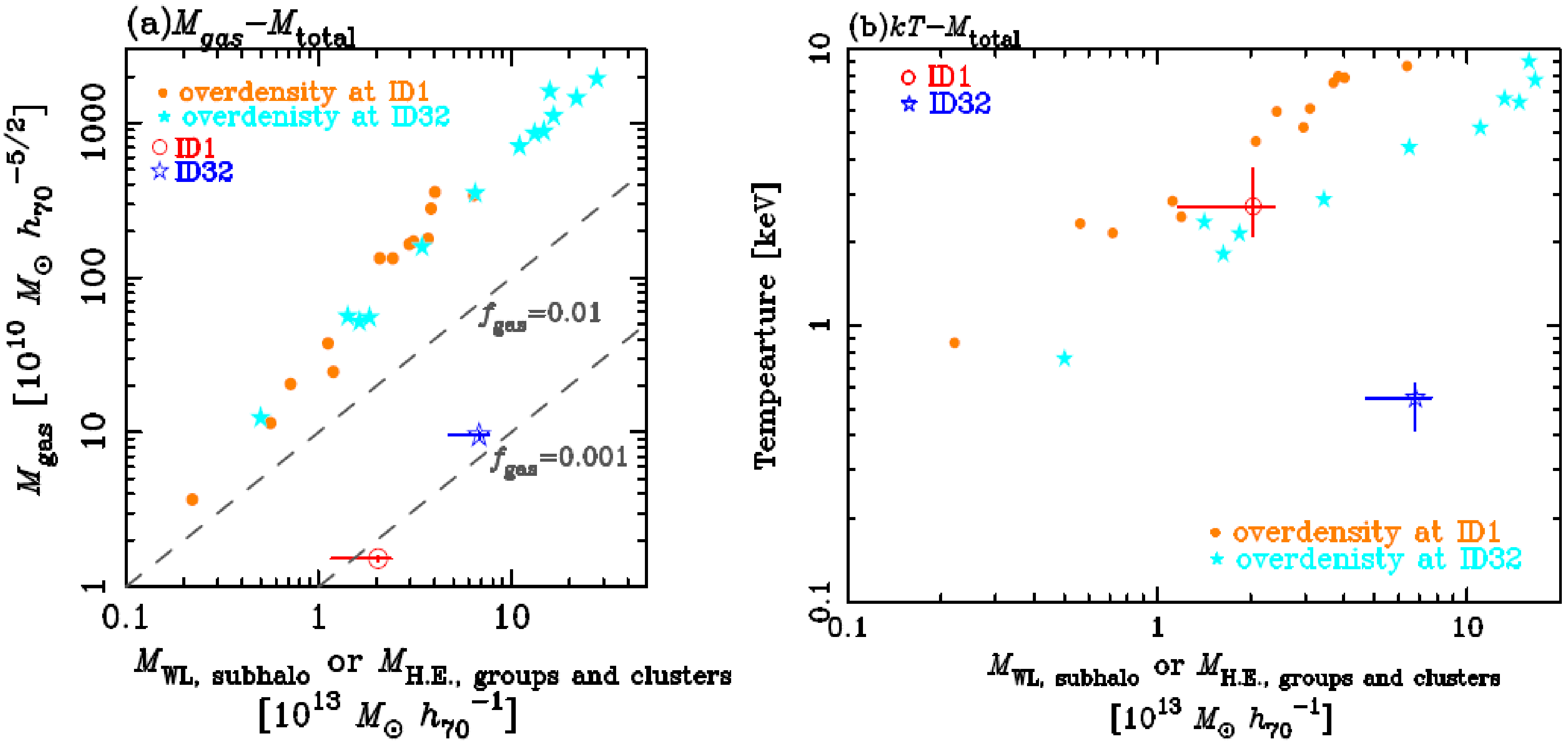

Mass-to-Light ratio

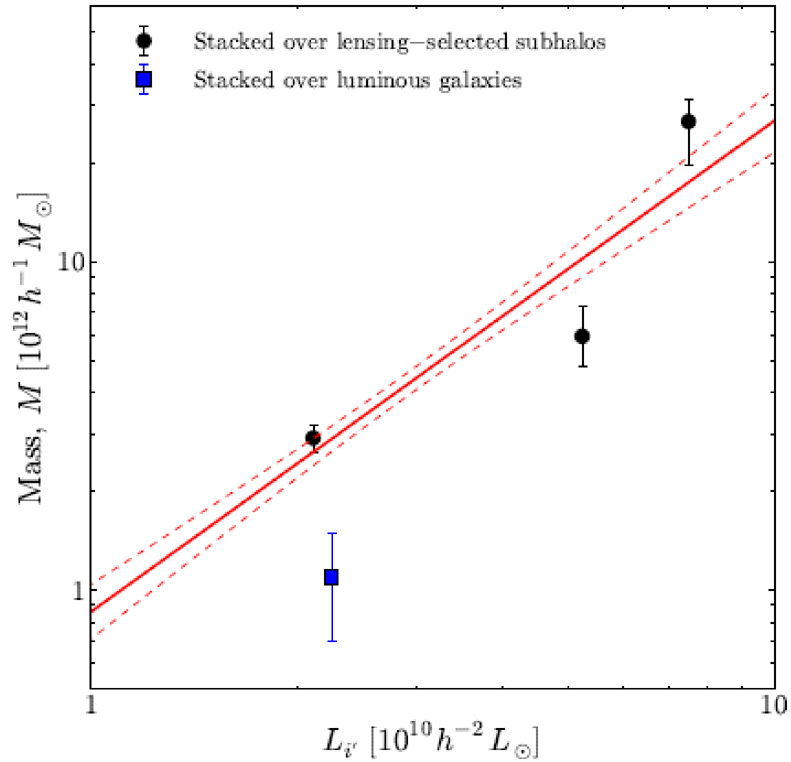

$$M/L = 86.1^{+18.1}_{-15.0}(L_{i'}/10^{10}h^{-2}L_{\odot})^{0.49\pm0.16}[hM_{\odot}/L_{i',\odot}]$$

$M_{\text{tot}} \propto L^{0.431\pm0.119}$ for simulated massive cluster at z = 0

Limousin et al. (2009)

$$M/L = (2.35 \pm 0.19)\left(L_I/10^{10}\,L_{I,}\right)^{0.32\pm0.06}$$

for the SAURON sample, Cappellari et al. (2006)

Observed Mass function of Subhalo

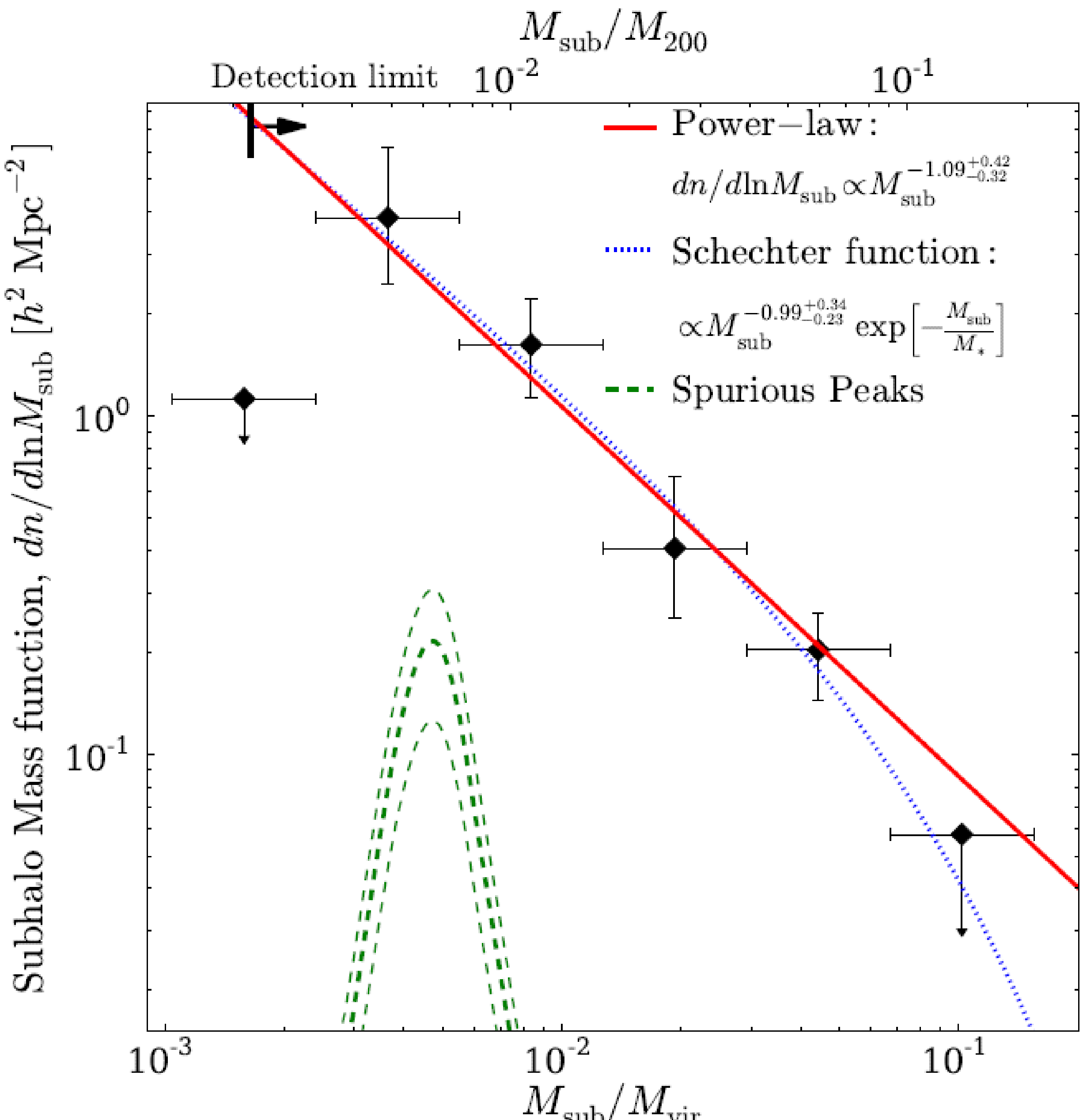

Power spectrum and Halo Mass function in WDM universe

R.E. Smith & K. Markovic, PRD 2002

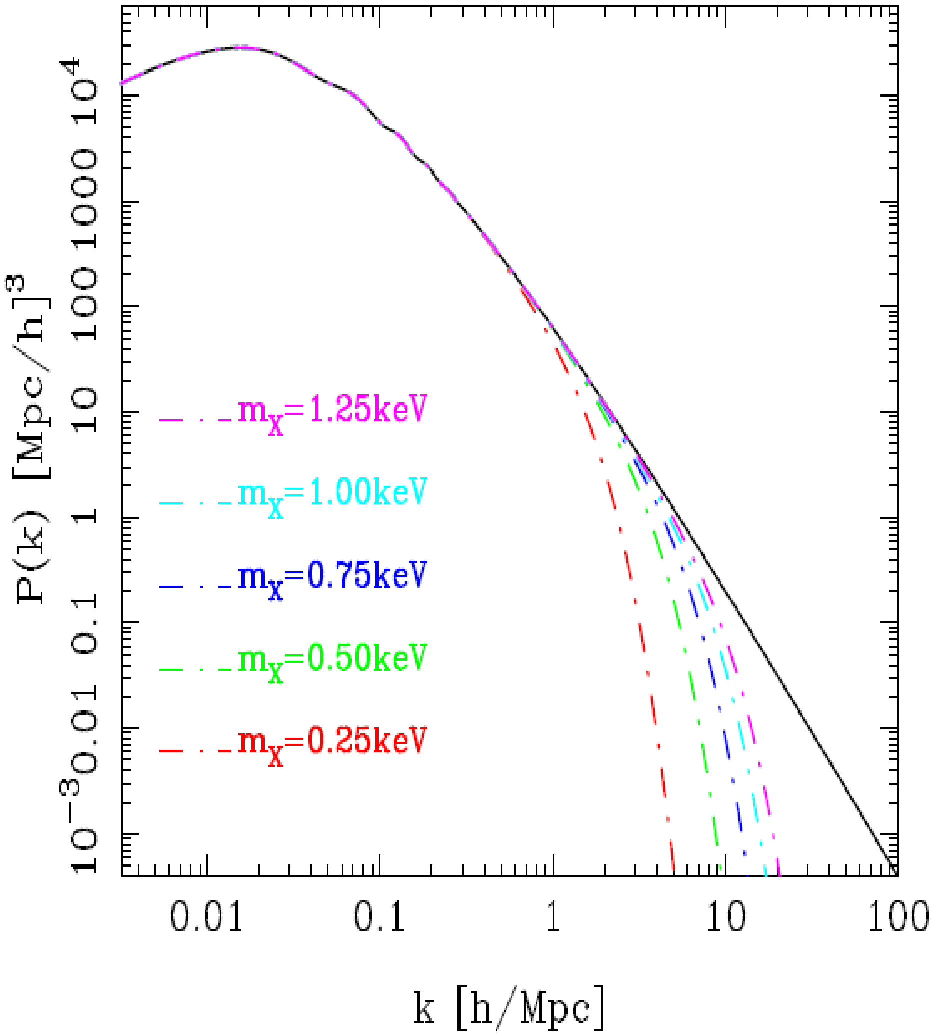

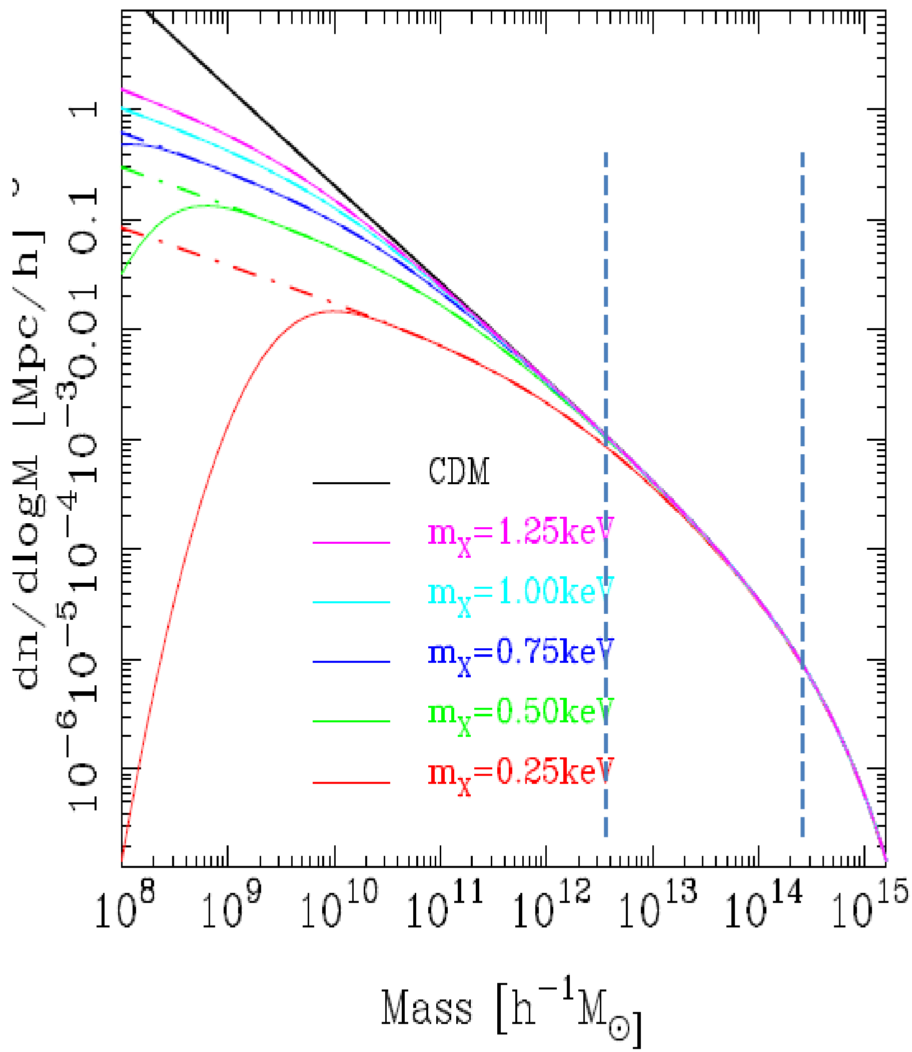

Classification of subhalos in mass and projected distance from the center

Sub-sample[a]	N_{sub}[b]	M_{sub}[c] $10^{12}h^{-1}M_\odot$	r_t[c] h^{-1}kpc	$\langle L_{i'}\rangle$[e] $10^{10}h^{-2}L_{i'}$
$-4.6 \times 10^{12}\ h^{-1}M_\odot$ †	21	$2.91^{+0.28}_{-0.29}$	$27.48^{+2.43}_{-1.91}$	2.11
$(4.6-10] \times 10^{12}\ h^{-1}M_\odot$	8	$5.93^{+1.43}_{-1.11}$	$72.79^{+25.42}_{-15.07}$	5.24
$10^{13}\ h^{-1}M_\odot$ − †	3	$26.72^{+4.28}_{-4.10-5.88}$	$161.15^{+57.25}_{-22.33}$	7.49
$0-20'$	11	$3.05^{+0.56}_{-0.58}$	$35.10^{+5.28}_{-4.26}$	5.35
$20'-40'$	10	$5.00^{+0.74}_{-0.65}$	$49.29^{+8.76}_{-7.66}$	3.47
$40'-60'$	8	$5.43^{+1.04}_{-1.33-0.73}$	$65.08^{+10.55}_{-19.51}$	1.52
$60'-80'$	3	$30.29^{+3.21}_{-3.23-1.75}$	$209.69^{+2.99}_{-13.29}$	6.16

Mean distortion profiles of the averaged subhalo in eah class

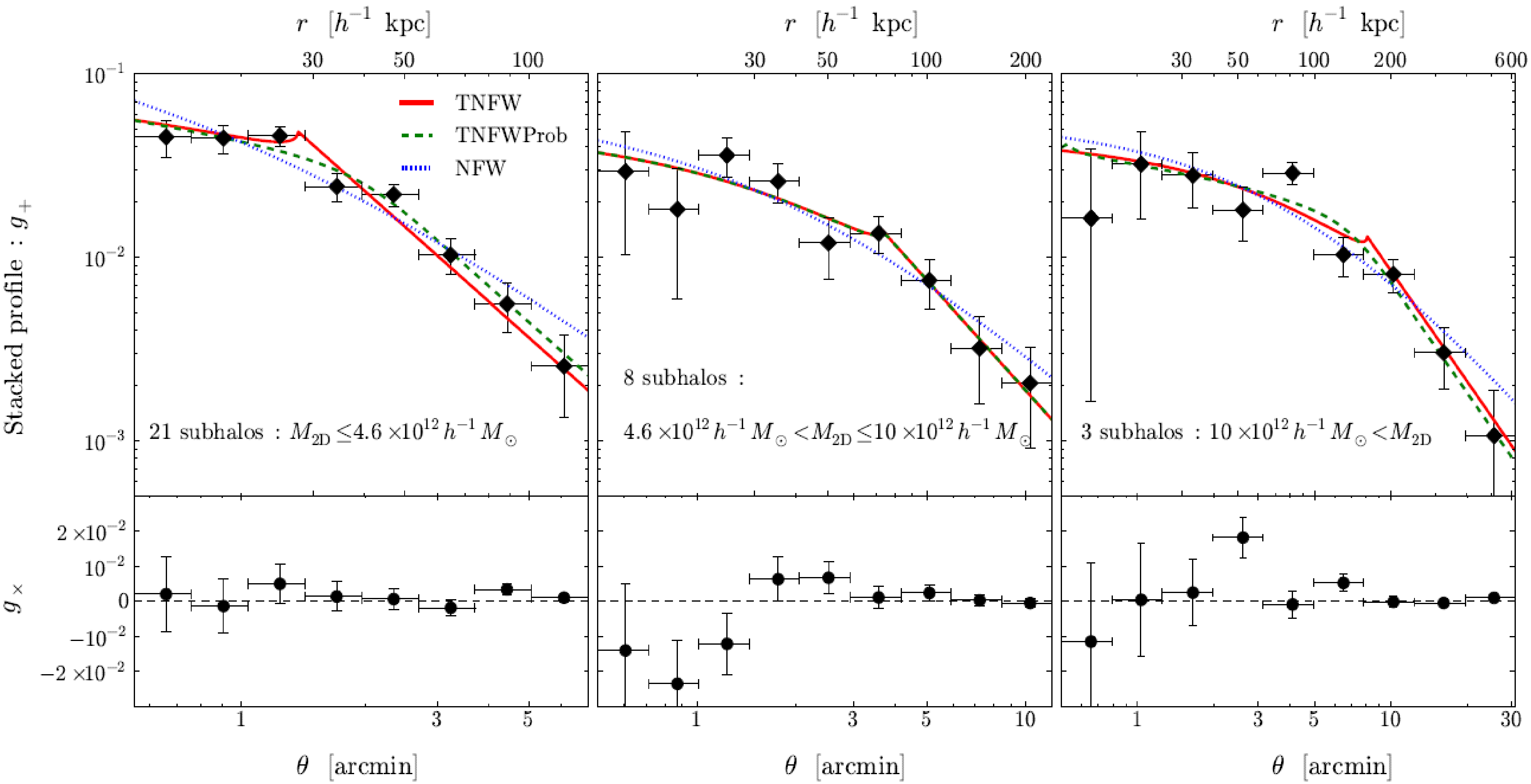

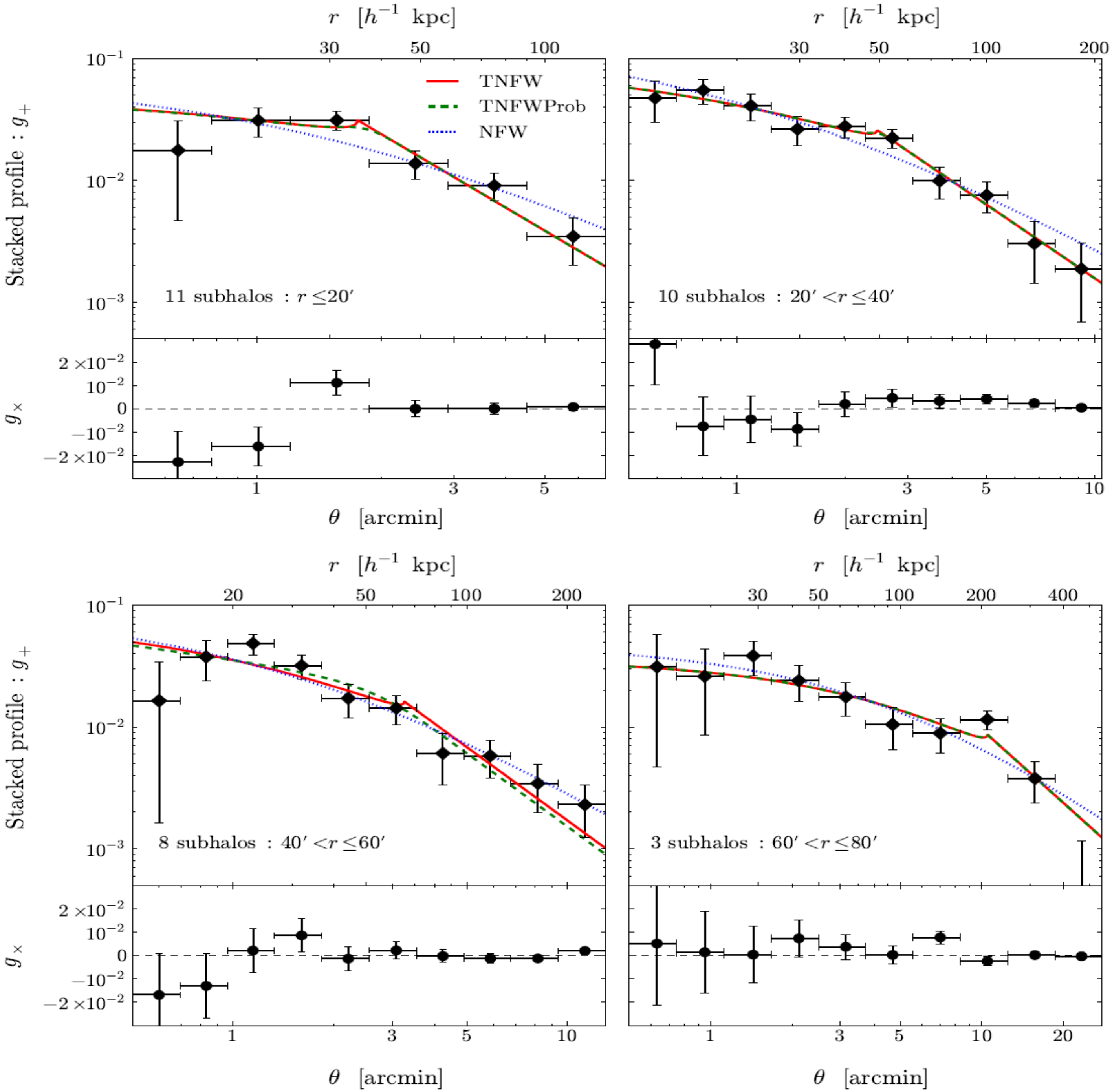

r [h⁻¹ kpc]
TNFW
TNFWProb
NFW
Stacked profile : g+
11 subhalos : r ≤20′
10 subhalos : 20′ <r ≤40′
8 subhalos : 40′ <r ≤60′
3 subhalos : 60′ <r ≤80′
g×
θ [arcmin]

Distance-dependence of subhalo size

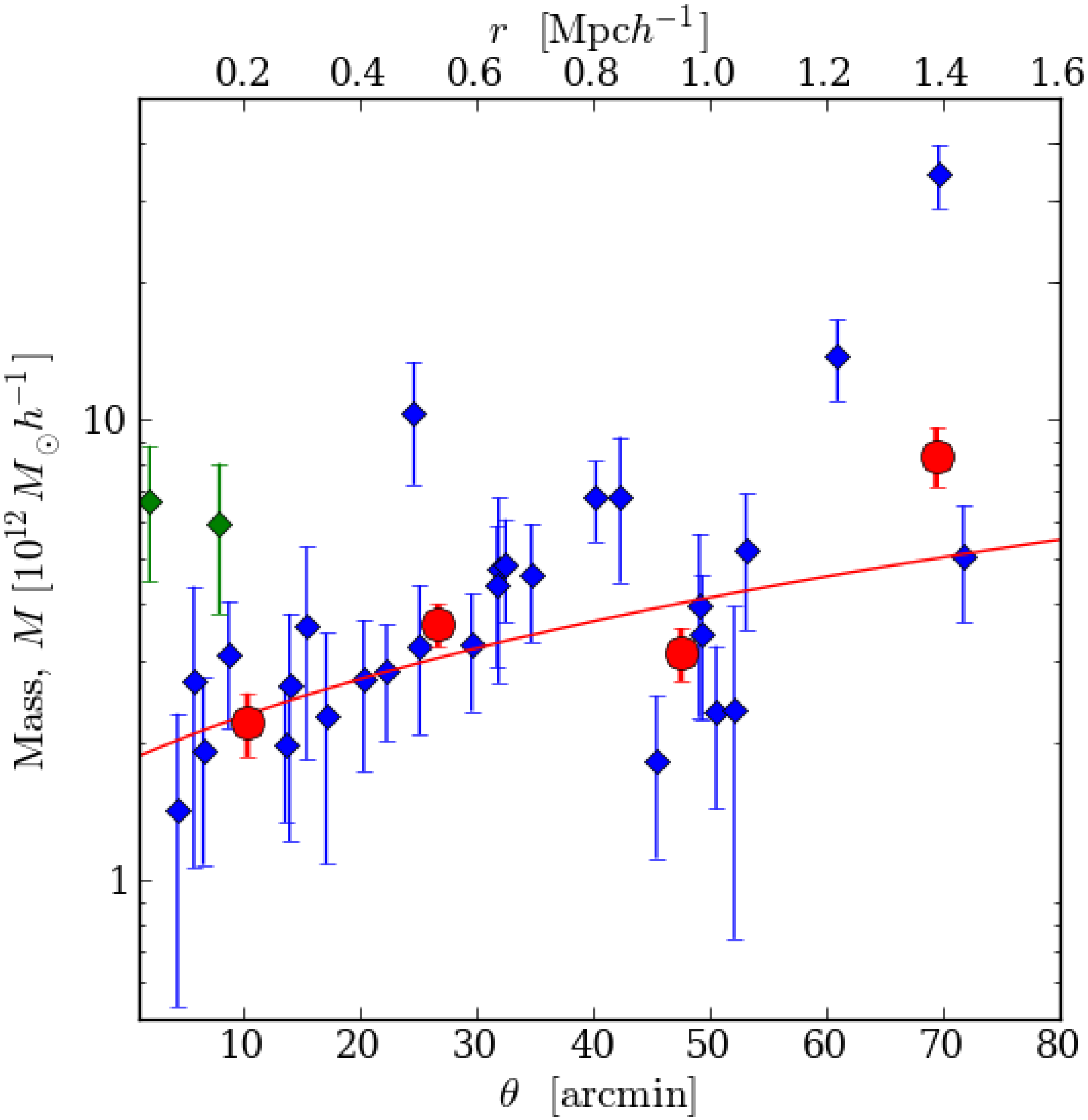

Main Halo

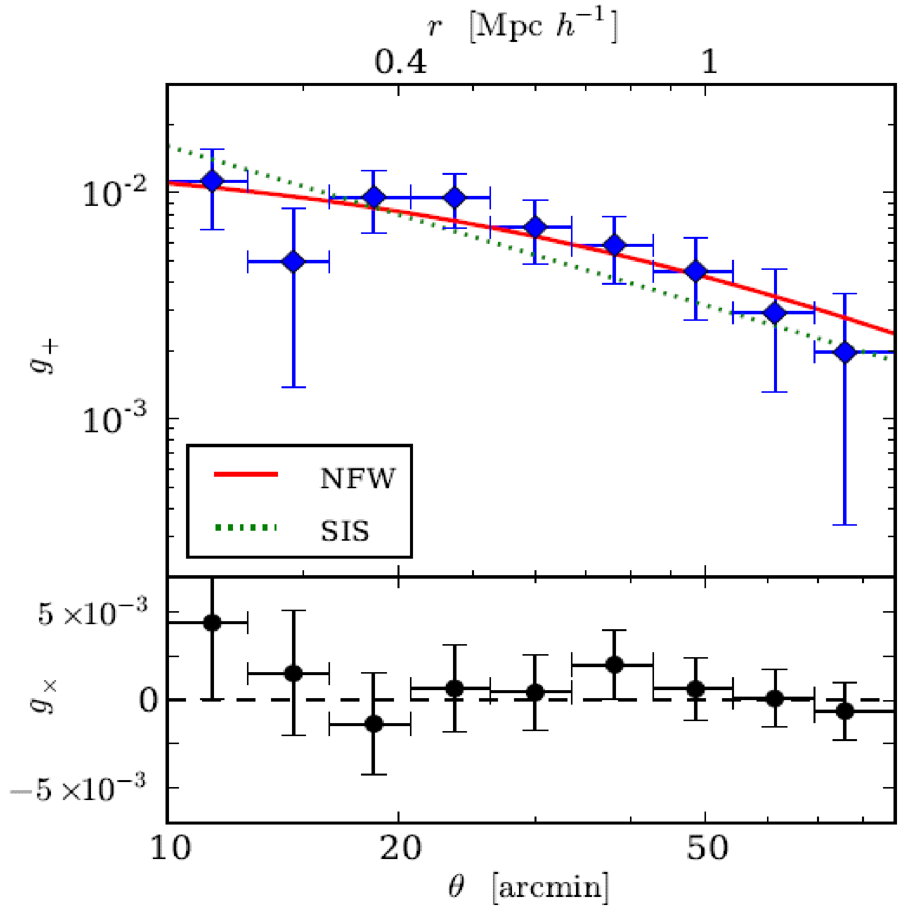

Fitting Method[a]	$M_{\rm vir}$ $10^{14}\ h^{-1}M_\odot$	$c_{\rm vir}$	M_{200} $10^{14}\ h^{-1}M_\odot$	c_{200}	M_{500} $10^{14}\ h^{-1}M_\odot$
g_+ profile	$8.42^{+4.17}_{-2.42}$	$3.57^{+1.54}_{-1.12}$	$6.23^{+2.53}_{-1.58}$	$2.55^{+1.17}_{-0.84}$	$3.89^{+1.04}_{-0.76}$
ζ_c profile	$8.31^{+2.42}_{-1.82}$	$3.24^{+0.80}_{-0.67}$	$6.08^{+1.51}_{-1.20}$	$2.30^{+0.61}_{-0.50}$	$3.67^{+0.69}_{-0.60}$

Total signal(main halo+subhalos+LSS)

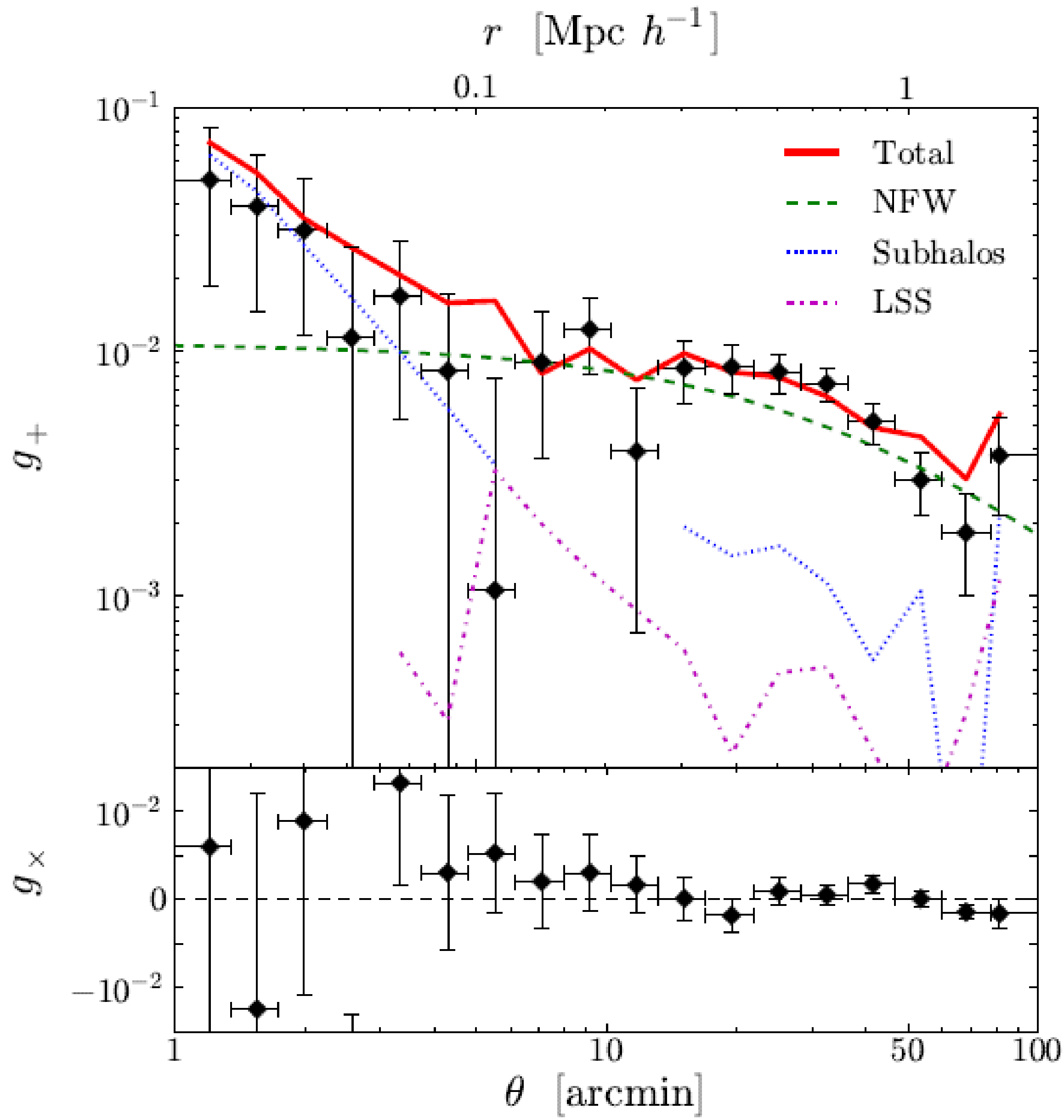

Possible Errors in our measurement

- Projection effect in mass estimate

  Effect from LSS

  Flexion observation may help

- Accidental peaks by Random shear distribution

  We generate shear randomly 200 times to see if peaks appear

  5.32±2.23 peaks are generated each time

  However mass profile is totally different from the lensing signal

- Def. of subhalo

  32 for S/N >3

  49 for S/N>2.75 and 24 for S/N>3.25

  Our condition is conservative in the sense that all the identified peak corresponds to galaxy group in cluster

Conclusion

- GL plays unique and important role in the observational cosmology
- We have found 32 DM subhalos in Come cluster($z=0.0236$) by weak lensing and measured their mass and size
- We constructed mass function of DM subhalos purely from observation and confirmed that it is consistent with CDM prediction.
- Distance dependence of the size of DM suhalo from the center of cluster can be understood as the result of tidal effect of main halo
- We also obtained the relation of DM subhalo mass and the luminosity of galaxies associated with DM subhalo

Above result has large statistical error because of small number of DM subhalo

Direction of Future Study

- 4-5 nearby clusters (z<0.05) can be observed by using HSC

  Number of DM subhalos will become of the order of 500 by observing about 20 nearby clusters
- Already 6 clusters are observe by HSC and is now analyzing the date

  RXC J0918.1-1205(ABELL0780) z=0.0539, RXC J0041.8-0918(ABELL0085) z=0.0555

  RXC J2205.6-0535(ABELL2415) z=0.0582, RXC J0056.3-0112 (ABELL0119) z=0.0442

  RXC J1921.1+4357(ABELL2319) z=0.0557, RXC J0319.7+4130(PERSEUS) z=0.0179
- It is very important to develop accurate bias free method of PSF correction to improve the accuracy of weak lensing analysis.
- More accurate estimate of LSS effect.

  Flexion measurement? (HOLICs. Y.Okura)
- Collaboration with Ｘ-ray and spectroscopic observation help us to study the formation of cluster in detail (very unfortunately HITOMI was failed.)

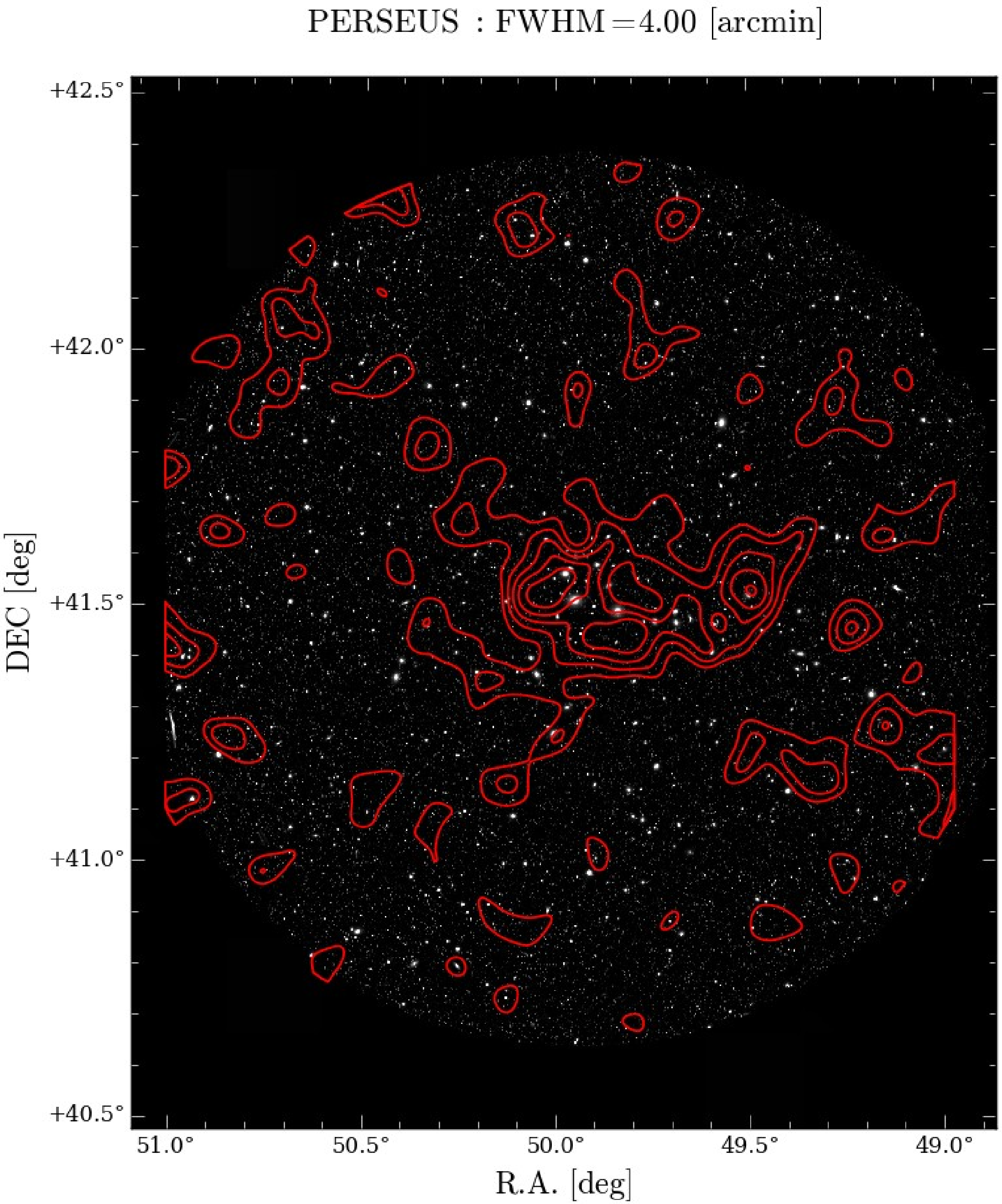
PERSEUS : FWHM = 4.00 [arcmin]
DEC [deg]
+42.5°
+42.0°
+41.5°
+41.0°
+40.5°
51.0°
50.5°
50.0°
49.5°
49.0°
R.A. [deg]

By N. Okabe